A Novel Patient-Specific Landmark-Guided Approach for Intramuscular Botulinum Neurotoxin Injections Into the Rotator Cuff: A Cadaveric Study

Dave Osinachukwu Duru[1,2] *, David Lee[1,2], Gavin E. Jarvis[3], Niel Kang[1,4], Salma Chaudhury[1,4], Cecilia Brassett[1].

[1]Human Anatomy Centre, Department of Physiology, Development and Neuroscience, University of Cambridge, Cambridge, UK
[2]Gonville & Caius College, University of Cambridge, Cambridge, UK
[3]School of Medicine, University of Sunderland, Sunderland, UK
[4]Department of Trauma and Orthopaedics, Cambridge University Hospitals NHS Foundation Trust, Cambridge, UK

*Corresponding author email address: dd614@cam.ac.uk (D.O. Duru),

Research was presented at the British Association of Clinical Anatomists (BACA) Summer Scientific Meeting on 4th July 2025 at Aston Medical School, Aston University, Birmingham, B4 7ET, UK.

At the scientific meeting, this work was awarded the **Conrad-Lewin Prize** for Best Oral Presentation.

Ethics: The donors had provided consent for anatomical research prior to decease in compliance with the Human Tissue Act 2004.
Data Availability Statement: The datasets generated and analysed during the current study are available from the corresponding author upon reasonable request.
Conflicts of interest: None
Funding: This work was funded in part by the Royal College of Surgeons of England Intercalated Bachelor of Science Degree in Surgery Award.
Acknowledgements: We sincerely thank the donors for enabling this cadaveric research to be possible. We also thank the Human Anatomy Dissection Room technical staff for their significant support and providing the necessary equipment to conduct this research.

A Novel Patient-Specific Landmark-Guided Approach for Intramuscular Botulinum Neurotoxin Injections Into the Rotator Cuff: A Cadaveric Study

Abstract

Background: Myofascial pain syndrome (MFPS) causes chronic shoulder pain. Supraspinatus and infraspinatus, rotator cuff muscles innervated by the suprascapular nerve, are commonly affected. Intramuscular botulinum neurotoxin (BoNT) injections near motor points (*i.e.,* visible nerve branch entry sites used as a proxy for motor endplates) are an effective treatment for such pain. However, current techniques limit accessibility. This study aimed to develop a patient-specific, landmark-guided technique for BoNT delivery into supraspinatus and infraspinatus using scapular dimensions.

Methods: Ten pairs of cadaveric shoulders (n=20) were dissected to identify supraspinatus and infraspinatus motor points. Distances from scapular landmarks to these motor points were measured in two axes. These distances were correlated with scapular dimensions (height, spine length, width) using linear regression. Patient-specific predictive formulae were derived. For validation, landmark-guided methylene blue dye injections were performed on four additional shoulders using calculated coordinates.

Results: For supraspinatus, motor points were predicted using deltoid tubercle and root of the scapular spine ($r = 0.58–0.64$, $p = 0.0016–0.021$). For infraspinatus, root of the scapular spine and lateral acromion were used ($r = 0.46–0.60$, $p = 0.0054–0.0500$). In all validation specimens, injected dye accurately reached the motor points.

Conclusion: This study provides a validated, patient-specific, landmark-guided technique for BoNT delivery into the rotator cuff, offering an approach for accessible analgesia.

Keywords: Rotator cuff, Botulinum neurotoxin (BoNT), Myofascial pain, Landmark-guided, Injection, Cadaveric, Suprascapular nerve, Variation, Patient-specific, Motor points

Introduction

Shoulder pain is prevalent, afflicting about 50% of the world's population each year (Brox, 2003). While its aetiology is multifactorial, a common cause is myofascial pain (Hains et al., 2010). Myofascial pain is characterised by hyperirritable trigger points – tender, taut bands of skeletal muscle – commonly located in the back, neck and shoulder (Epstein et al., 2018; Gilchrist and Pokorná, 2021).

Within the shoulder, myofascial trigger points (MTrPs) often involve the rotator cuff muscles (Perez-Palomares et al., 2009). In particular, 60–68% of myofascial shoulder pain cases involve supraspinatus, with 78% involving infraspinatus (Bron et al., 2011; Villafañe et al., 2019). Electrophysiological analyses suggest MTrPs tend to localise near motor points (Chu, 1995; Simons et al., 2002). In this study, we define motor points as the visible entry sites of suprascapular nerve branches into the muscle belly, which serve as a practical anatomical proxy for underlying motor endplates (Harrison et al., 2007). Within the rotator cuff, MTrPs cause significant pain, limit range of motion, and diminish quality of life (Villafañe et al., 2019).

Myofascial pain can be managed by physiotherapy, topical vapocoolants or local injections of corticosteroids, lidocaine, or botulinum neurotoxin (BoNT) (Cheshire et al., 1994; Shin et al., 2014; Xie et al., 2015; Kang et al., 2019).

BoNT inhibits acetylcholine release at the neuromuscular junction, producing prolonged muscle relaxation to relieve myofascial pain (Cheshire et al., 1994; De Andrés et al., 2003). Targeting BoNT injections closer to motor points improves efficacy (Miguel and Cirera, 2021); however, this remains technically challenging due to extensive variation in their topography between patients (Lee et al., 2022, 2023). This variation also underscores a need for personalised approaches to injection targeting.

Current BoNT injection protocols rely on ultrasound or electromyography guidance (Evans and Porter, 2015; Tan and Jia, 2021). While effective, these techniques are not

universally available and require specialist training. This highlights a clinical use for anatomically validated, landmark-guided injection approach.

This cadaveric study presents image-free, patient-specific approaches for landmark-guided BoNT injection into supraspinatus and infraspinatus, targeting motor points. These approaches, informed by scapular dimensions, were validated through blind injection of methylene blue.

2. Materials and Methods

2.1 Specimen preparation

Ten pairs of cadaveric shoulder specimens (n=20) were provided by [redacted] The donors (5 male, 5 female; mean (*SD*) age = 80.8 (8.9) years) had provided consent for anatomical research prior to decease in compliance with the Human Tissue Act (2004). The donors were preserved by cannulation of the common carotid or femoral artery, and injection under pressure of a solution containing 38% ethanol, 1.5% methanol, 4.2% formaldehyde, and 56.3% distilled water.

2.2 Defining scapular landmarks

The shoulder specimens were dissected to reveal six bony scapular landmarks: 1) superior angle; 2) inferior angle; 3) root of the scapular spine; 4) deltoid tubercle; 5) lateral acromion (defined as the mid-aspect of the lateral edge of the acromion in line with the axis of the patient's scapular spine); and 6) acromioclavicular (AC) joint (Figure 1). These landmarks were selected for their consistent bony morphology and ease of surface palpation.

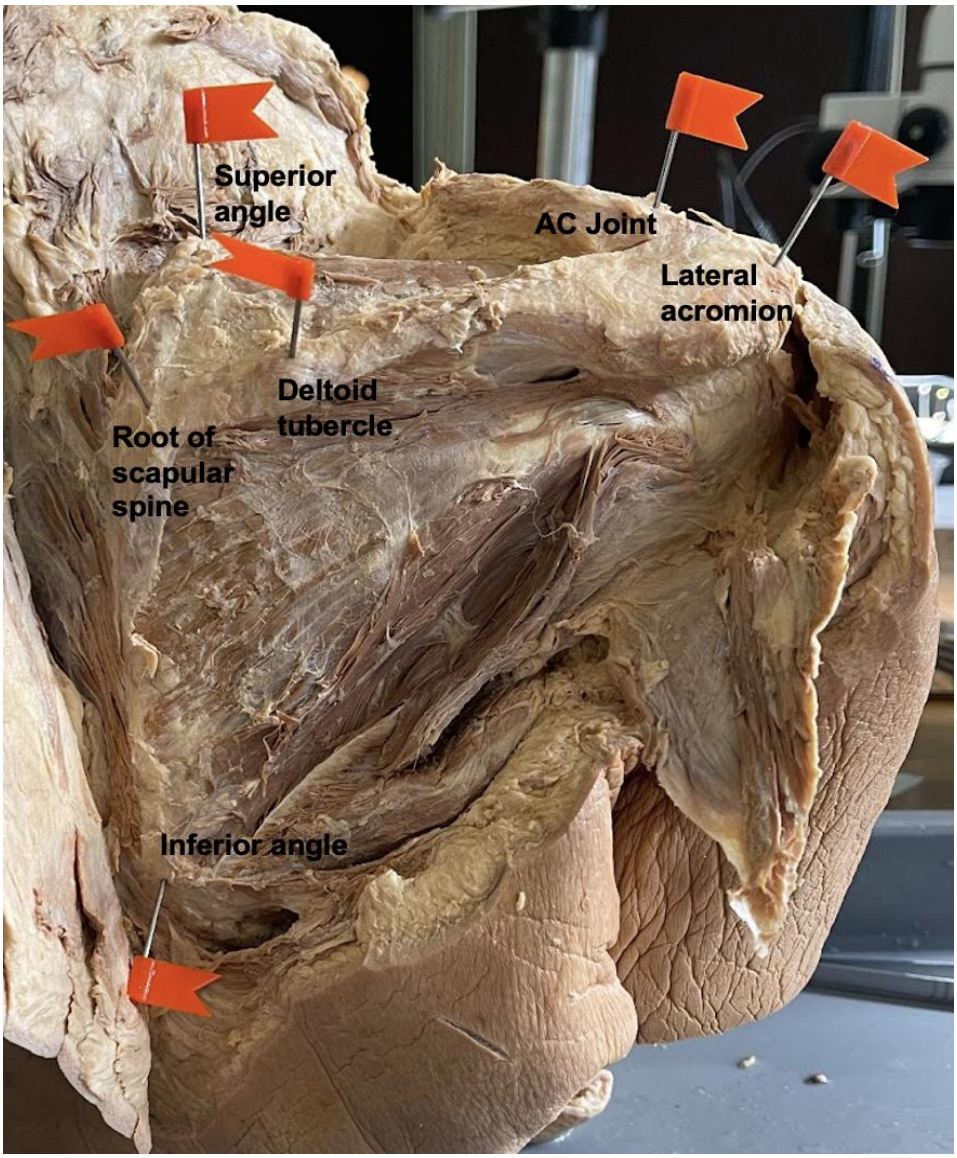

Figure 1. Bony scapular landmarks

Six bony scapular landmarks of interest, used to guide injections into supraspinatus and/or infraspinatus. [Posterior view of right shoulder]

2.3 Measuring scapular dimensions

Scapular dimensions were measured, including scapular height, spine length, and width (Figure 2).

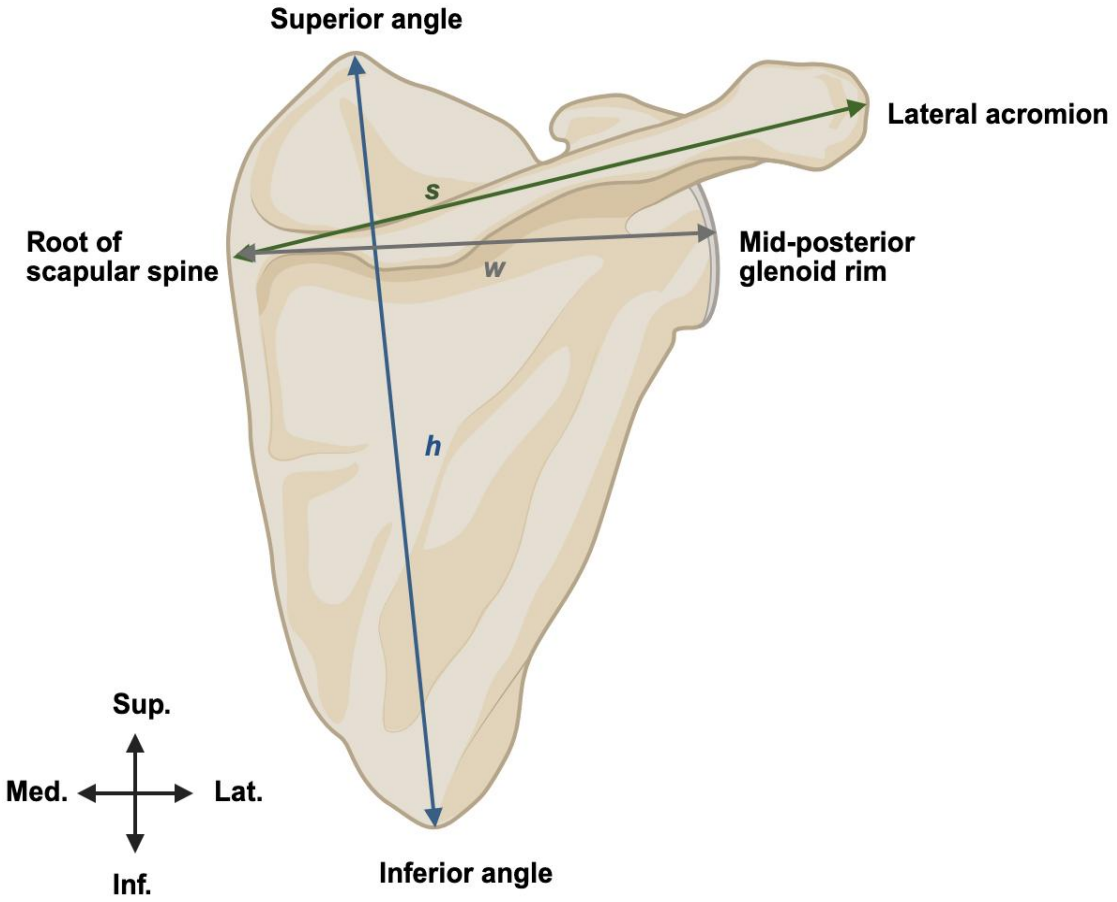

Figure 2. Measurement of scapular dimensions

Schematic figure of the posterior view of a right scapula.

Height (h) = distance from the superior angle to inferior angle.

Spine length (s) = distance from the root of the spine to the lateral acromion.

Width (w) = distance from the root of the spine to the mid-posterior glenoid rim.

Key: Sup., superior; Inf., inferior; Med., medial; Lat., lateral. [Figure made with BioRender]

2.4 Defining key points of interest

Specimens were further dissected to visualise suprascapular nerve motor branch insertions into supraspinatus and infraspinatus. The muscles were reflected, and pins

were inserted perpendicular to the underlying scapular bone surface to mark motor branch entry. The muscles were then laid into their *in situ* positions, as the nerve enters the muscle belly close to the bone (Figure 3).

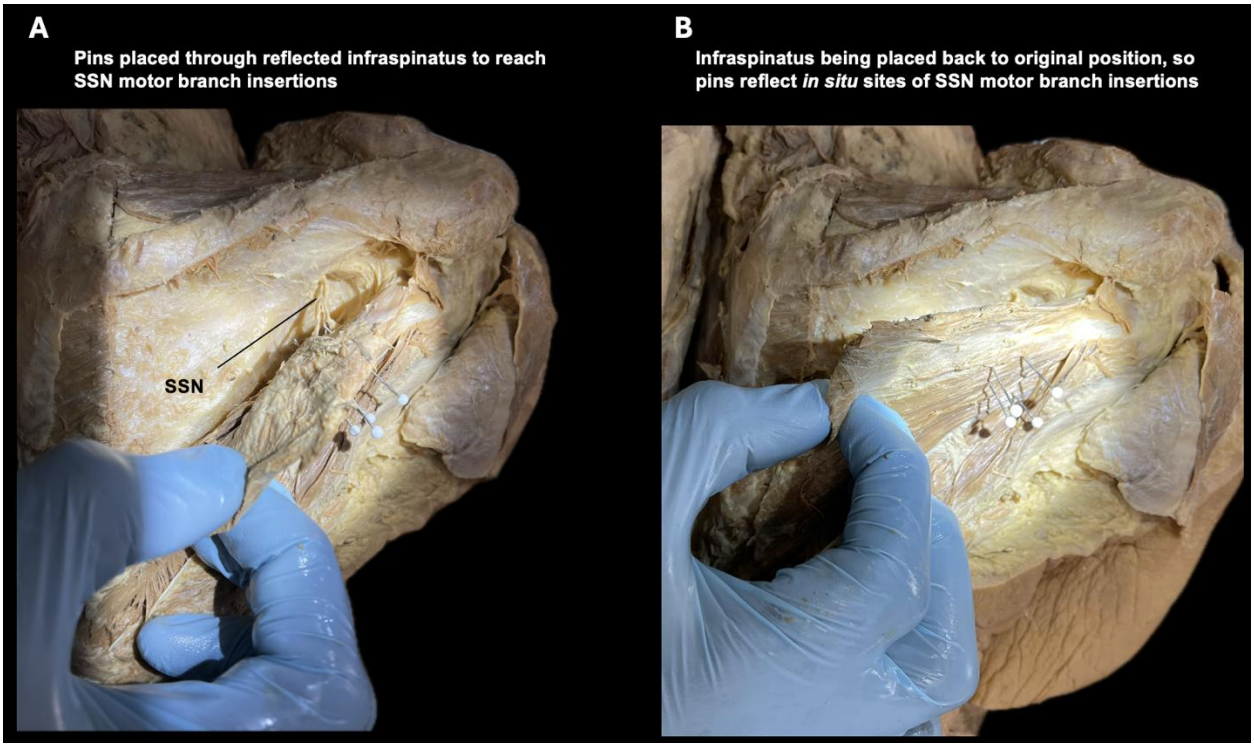

Figure 3. Identifying suprascapular motor nerve insertions into infraspinatus (motor points)

Defining sites of suprascapular nerve (SSN) motor branch entry into infraspinatus via reflection and pin placement.

2.5 Measuring supraspinatus and infraspinatus motor point topography

Distances (mm) were measured along two axes for each of the muscles via ruler-calibrated images and *ImageJ* software. Given the variable contours of musculature and the alterations with formalin fixation, a defined two dimensional plane was transposed over the supraspinatus and infraspinatus to inform distance measures; X (medial-lateral) and Z (anterior-posterior) distances from the average site of nerve entry into supraspinatus were measured from: 1) acromioclavicular joint (AC); 2) superior angle (SA); 3) root of the scapular spine (RS); 4) deltoid tubercle (DT); and 5) lateral acromion (LA; exemplified in Figure 4A).

X (medial-lateral) and Y (superior-inferior) distances from landmarks to the average site of nerve entry into infraspinatus were measured from: 1) root of the scapular spine (RS); 2) inferior angle (IA); 3) deltoid tubercle (DT); and 4) lateral acromion (LA; exemplified in Figure 4B).

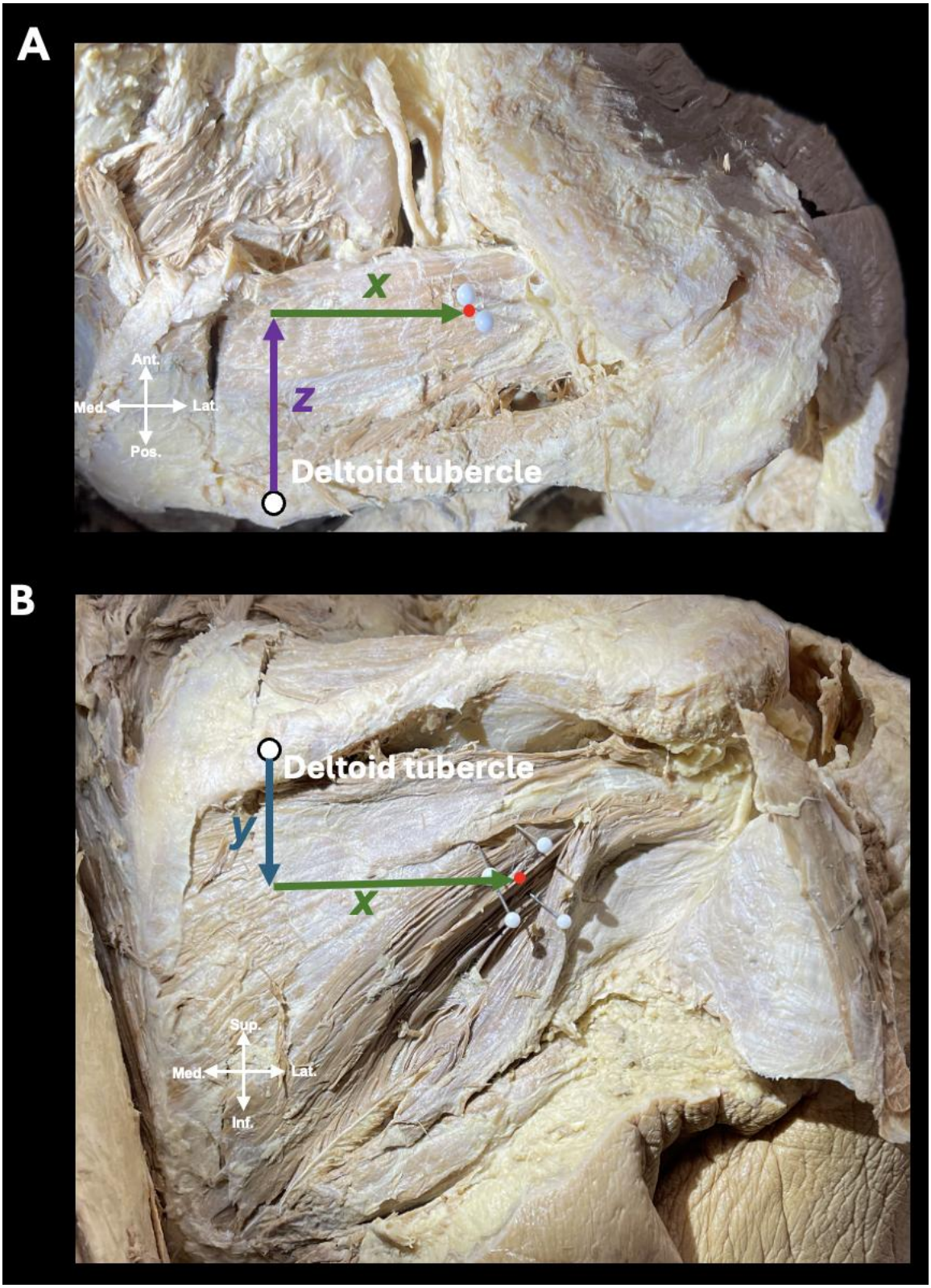

Figure 4. Measurement of distances from deltoid tubercle to average site of motor nerve entry into A) supraspinatus and B) infraspinatus

Distance measures in two axes from the deltoid tubercle to the injection target of A) supraspinatus [superior view of right shoulder with trapezius reflected] and B) infraspinatus [posterior view of the right shoulder with deltoid reflected]. In A) X mm reflects the medial-lateral distance and Z mm reflects the anterior-posterior distance. In B) X mm reflects the medial-lateral distance and Y mm reflects the superior-inferior distance. The red dot is equidistant from the pin placements that delineate sites of motor points; the rationale is that with a single injection localised near the sites of suprascapular nerve motor entry, sufficient coverage can be achieved, relieving myofascial pain.

The specimens were placed in identical positions, guided by demarcations on a board and camera placement was the same for all specimens, enabling consistency (Figure 5).. The accuracy of image-based measures was confirmed with in-person digital caliper measures performed in triplicate by a single experimenter and performed blinded by a second experimenter.

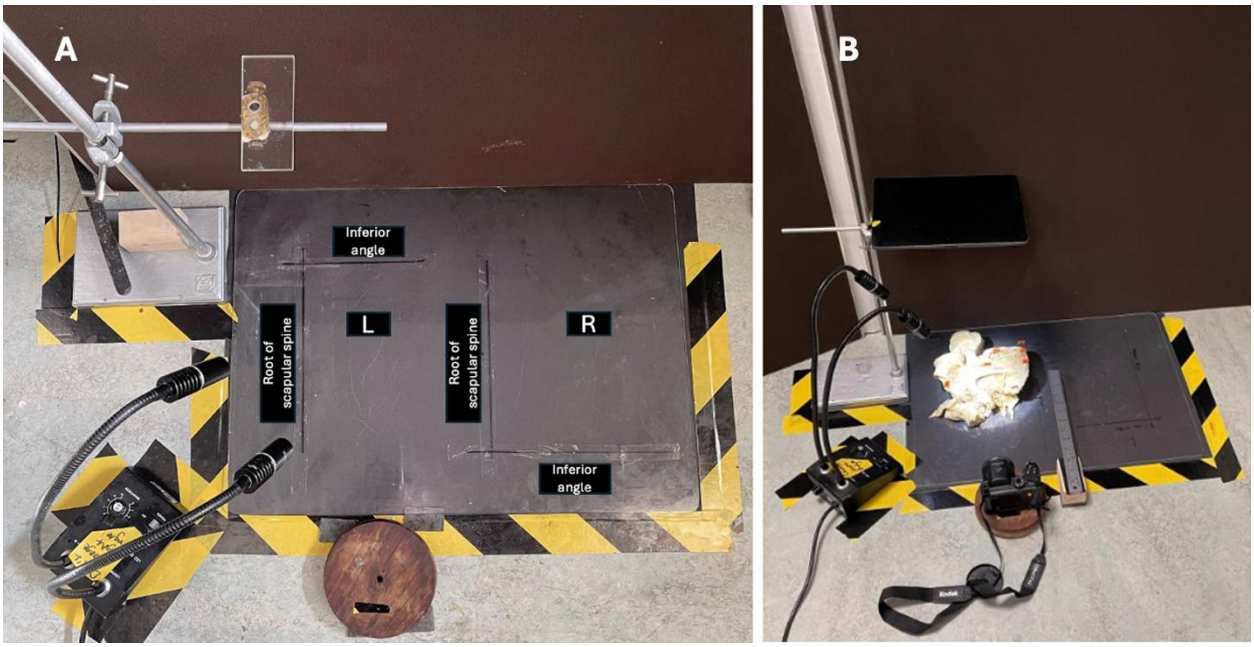

Figure 5. Experimental apparatus

L= left shoulder and R=right shoulder

2.6 Statistical analysis

Graphs were produced using Prism v10.4.2 (GraphPad). Statistical analyses were conducted using Prism and Microsoft Excel v16.95.4. Sample size is n=20 throughout. The n-value represents the number of shoulder specimens involved in the analyses. To test for normal distribution, the Shapiro-Wilk test (Shapiro and Wilk, 1965) and Q-Q plots were used. Simple linear regression analysis was employed to test for correlation between variables, measured by R^2 and the Pearson correlation coefficient (r). The F-test was used to investigate for statistically significant, non-zero relationships between variables. Statistical significance was attributed to differences for *p*-values ≤0.05 (*$p \leq 0.05$).

2.7 Dye injection validation

To validate the accuracy of landmark-guided localisation of motor points, injection via a 25-gauge needle of 2.5 mL of 0.25% methylene blue dye solution was performed on 4 additional unpaired formalin-fixed shoulder specimens (2 right, and 2 left), with the skin attached. The specific approach to performing these validating injections was derived from the *Results*. Following injection, the specimens were dissected to assess for coverage of motor points.

The volume and needle size were selected to resemble ultrasound- and electromyography-guided injections in clinical practice (Tan and Jia, 2021; Kyu-Ho et al., 2023); however, as no consensus guidelines for supraspinatus or infraspinatus have been reported to date, the volume of injectate and needle size were informed by other rotator cuff muscles, such as subscapularis.

3. Results

Measures of scapular dimensions (Table 1) and distances from landmarks to the average supraspinatus (Table 2) and infraspinatus (Table 3) motor points were performed on 20 shoulder specimens (10 pairs). A mean of 2.11 ± 0.32 (range: 2–3) motor points were identified in supraspinatus, and 3.55 ± 0.62 (range: 2–5) in infraspinatus.

There was variation in scapular size but no significant left vs. right differences (two-tailed paired *t*-test; p>0.05).

Table 1. Measurement of scapular dimensions

	All specimens	**Left side**	**Right side**
Height	145.80 ± 15.19 (111.06–166.86)	147.61 ± 15.56	143.99 ± 15.42
Spine length	140.32 ± 14.31 (114.41–160.91)	137.87 ± 16.30	142.77 ± 12.37
Width	107.57 ± 12.43 (85.04–129.70)	106.58 ± 12.28	108.91 ± 13.13

All measurements are in mm (mean ± SD). The range of measurements between the different shoulder specimens is indicated in brackets.

There was variation in distances from landmarks to suprascapular nerve motor points, even between left and right shoulders for certain relations (Tables 2 and 3).

Table 2. X and Y distances from average location of supraspinatus motor points (SSNs) to scapular landmarks

Relation	All specimens	Left side	Right side
X AC–SSNs	48.19 ± 13.14 (27.77–70.34)	50.89 ± 15.32	45.49 ± 10.67
Z AC–SSNs*	16.24 ± 11.71 (-4.74–33.59)	13.62 ± 12.32	18.86 ± 11.06
X SA–SSNs	57.09 ± 15.37 (36.14–97.08)	53.88 ± 11.73	60.31 ± 18.39
Z SA–SSNs	17.28 ± 10.1 (3.32–37.56)	20.56 ± 12.66	14.0 ± 5.6
X RS–SSNs	66.56 ± 16.2 (47.92–111.3)	65.14 ± 12.71	67.98 ± 19.7
Z RS–SSNs*	0.15 ± 8.2 (-17.53–14.0)	-1.16 ± 10.48	1.45 ± 5.33
X DT–SSNs	33.03 ± 12.21 (15.93–57.56)	30.67 ± 12.81	35.39 ± 11.77
Z DT–SSNs	20.69 ± 8.5 (2.49–32.31)	17.93 ± 8.88	23.45 ± 7.54
X LA–SSNs	69.19 ± 13.49 (48.21–91.74)	70.98 ± 16.26	67.39 ± 10.62
Z LA–SSNs	27.89 ± 10.93 (7.51–45.35)	23.08 ± 11.27	32.71 ± 8.57

X AC–SSNs: medial distance from the acromioclavicular joint to the average supraspinatus motor point

Z AC–SSNs: anterior distance from the acromioclavicular joint to the average supraspinatus motor point*

X SA–SSNs: lateral distance from the superior angle to the average supraspinatus motor point

Z SA–SSNs: posterior distance from the superior angle to the average supraspinatus

motor point

X RS–SSNs: lateral distance from the root of the scapular spine to the average supraspinatus motor point

Z RS–SSNs: anterior distance from the root of the scapular spine to the average supraspinatus motor point*

X DT–SSNs: lateral distance from the deltoid tubercle to the average supraspinatus motor point

Z DT–SSNs: anterior distance from the deltoid tubercle to the average supraspinatus motor point

X LA–SSNs: medial distance from the lateral acromion to the average supraspinatus motor point

Z LA–SSNs: anterior from the lateral acromion to the average supraspinatus motor point

*All values are in mm and mean ± SD (range). Note that * indicate two relations with negative values. Typically, average motor nerve entry into supraspinatus (SSNs) was anterior to the AC joint and root of scapular spine (positive). In cases where these distances are negative, the average motor nerve entry into supraspinatus was posterior to the root of scapular spine or AC joint. X indicates medial-lateral distance and Y indicates anterior-posterior distance.*

Table 3. X and Y distances from average location of infraspinatus motor points (SSNi) to scapular landmarks

	All specimens	**Left side**	**Right side**
X RS–SSNi	67.65 ± 11.09 (48.31–83.83)	65.61 ± 12.72	69.68 ± 9.41
Y RS–SSNi	21.38 ± 10.29 (2.94–42.06)	22.33 ± 7.66	20.44 ± 12.76
X IA–SSNi	49.99 ± 12.05 (28.43–76.31)	45.26 ± 9.51	54.71 ± 12.90
Y IA–SSNi	80.46 ± 10.69 (62.34–100.35)	81.30 ± 13.31	79.62 ± 7.92
X LA–SSNi	68.89 ± 10.27 (53.39–88.31)	68.84 ± 9.86	68.94 ± 11.20
Y LA–SSNi	48.51 ± 11.28 (29.89–76.99)	47.41 ± 14.01	49.62 ± 8.34
X DT–SSNi	37.13 ± 10.52 (19.45–60.43)	37.18 ± 12.82	37.08 ± 8.32
Y DT–SSNi	25.89 ± 8.82 (6.87–41.04)	27.67 ± 8.25	24.11 ± 9.43

X RS–SSNi: Lateral distance from root of scapular spine to average infraspinatus motor point

Y RS–SSNi: Inferior distance from root of scapular spine to average infraspinatus motor point

X IA–SSNi: Lateral distance from inferior angle to average infraspinatus motor point

Y IA–SSNi: Superior distance from inferior angle to average infraspinatus motor point

X LA–SSNi: Medial distance from lateral acromion to average infraspinatus motor point

Y LA–SSNi: Inferior distance from lateral acromion to average infraspinatus motor point

X DT–SSNi: Lateral distance from deltoid tubercle to average infraspinatus motor point

Y DT–SSNi: Inferior distance from deltoid tubercle to average infraspinatus motor point

All values are in mm and mean ± SD (range). Summary table of the topographical relations of the average suprascapular nerve motor entry into infraspinatus (SSNi), the injection target, in the X (medial-lateral) and Y (superior-inferior) axes.

Simple linear regression assessed if there was a correlation between distance measures and scapular dimensions. Lateral distance from the superior angle to average supraspinatus motor point can be predicted by scapular height (r = 0.53; Figure 6A), spine length (r = 0.57; Figure 6B), or width (r = 0.52; Figure 6C). Lateral distance from the root of scapular spine to the average motor point may also be predicted by scapular height (r = 0.60; Fig 6A), spine length (r = 0.57; Figure 6B), or width (r = 0.51; Figure 6C). Based on spine length (r = 0.60; Figure 6B) or width (r = 0.66; Fig 6C), the anterior distance from the deltoid tubercle to the average motor point may be predicted. These findings indicate that the variable topography of supraspinatus motor points can be predicted using patient-specific scapular dimensions.

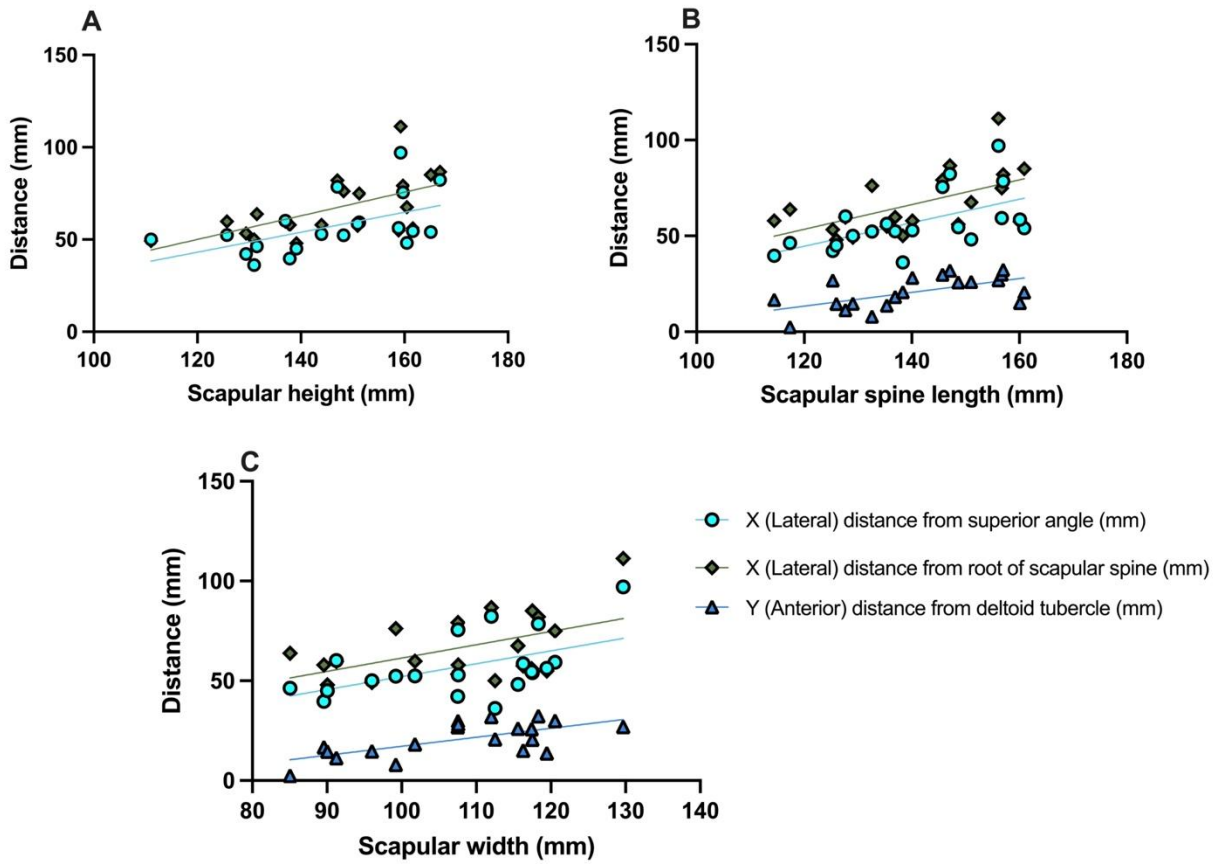

Figure 6. The topographical relations of supraspinatus motor points can be predicted by scapular dimensions

The topographical relations of supraspinatus motor points can be predicted by scapular dimensions. Scatter plot showing significant correlations between X and Z distances to the average motor nerve entry into supraspinatus and scapular A) height, B) spine length, and C) width.

Table 4. Linear regression line of best fit equations, R^2, and *p*-values from plots in Figure 6

Graph	Distance (X/Y) from landmark to injection site vs. scapular dimension	Line of best fit equation	R^2	*p*-value
A	X SA–SSNs vs. height	Y = 0.5409*X - 21.78	0.2858	0.0152
	X RS–SSNs vs. height	Y = 0.6402*X - 26.77	0.3603	0.0051
B	X SA–SSNs vs. spine length	Y = 0.6131*X - 28.93	0.3256	0.0086
	X RS–SSNs vs. spine length	Y = 0.6444*X - 23.85	0.3238	0.0088
	Z DT–SSNs vs. spine length	Y = 0.3595*X - 29.76	0.3660	0.0047
C	X SA–SSNs vs. width	Y = 0.6460*X - 12.51	0.2729	0.0181
	X RS–SSNs vs. width	Y = 0.6672*X - 5.320	0.2621	0.0210
	Z DT–SSNs vs. width	Y = 0.4511*X - 27.91	0.4350	0.0016

X SA–SSNs: lateral distance from the superior angle to the average supraspinatus motor point

X RS–SSNs: lateral distance from the root of the scapular spine to the average supraspinatus motor point

Z DT–SSNs: anterior distance from the deltoid tubercle to the average supraspinatus motor point

Summary statistics of simple linear regression analysing the relationship between the average motor nerve entry into supraspinatus (SSNs) and scapular dimensions.

Based on scapular height, the lateral (r = 0.60; Figure 7A) and inferior (r = 0.46; Figure 7A) distances from the root of the scapular spine to the average infraspinatus motor point can be predicted. Based on scapular spine length or width, the medial (r = 0.44–0.58; Figures 7B-C) and inferior (r = 0.50–0.58; Figures 7B-C) distances from the lateral acromion to the average infraspinatus motor point can be predicted. This suggests that the topography of infraspinatus motor points can be predicted by scapular dimensions.

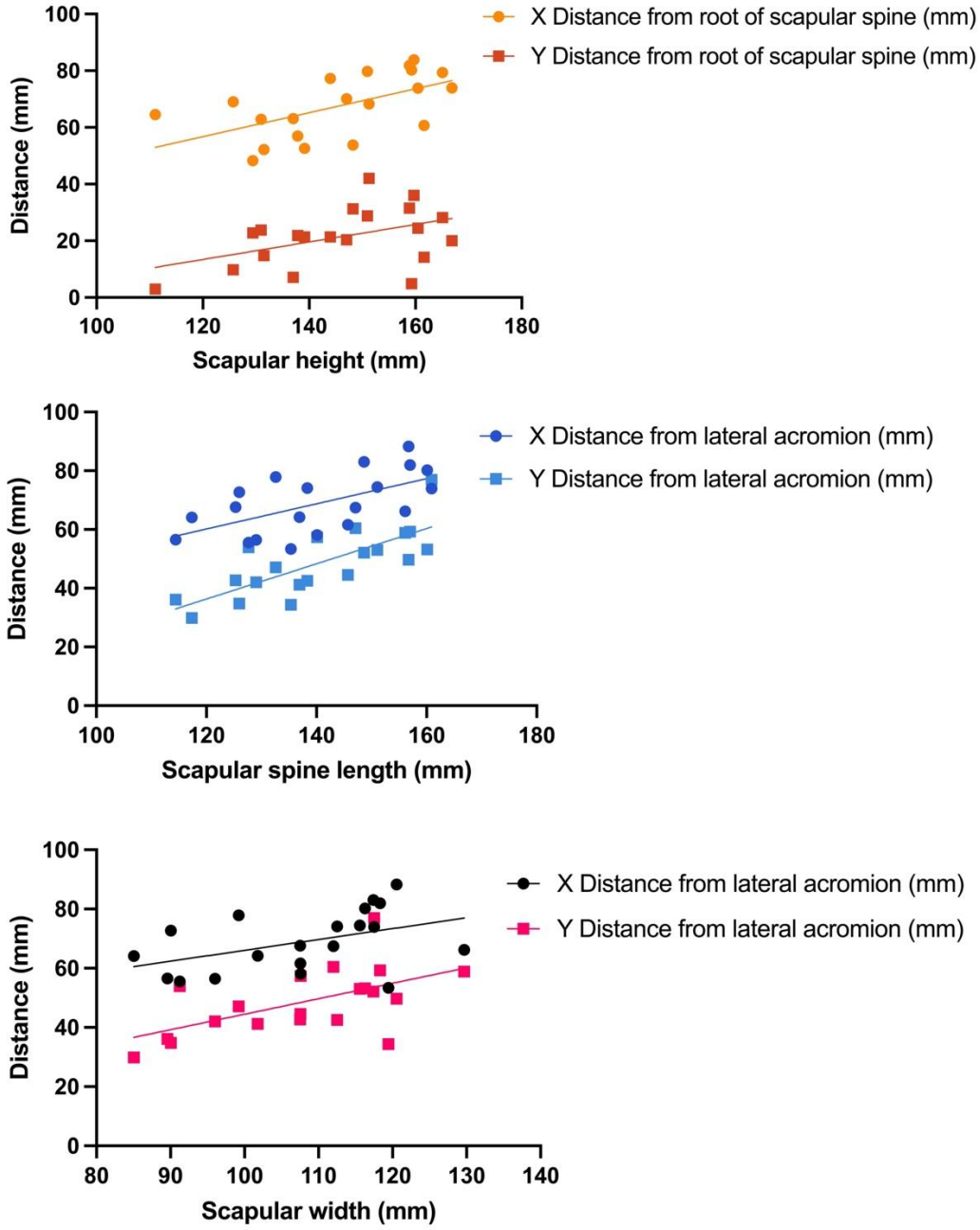

Figure 7. The topographical relations of infraspinatus motor points can be predicted by scapular dimensions

For the lateral acromion, X distance is medial, and Y is inferior. For the root of scapular spine, X distance is lateral, and Y is inferior.

Table 5. Linear regression line of best fit equations, R^2, and *p*-values from plots in Figure 7

Graph	Distance (X/Y) from landmark to injection site vs. Scapular dimension	Line of best fit equation	R^2	*p*-value
A	X RS–SSNi vs. height	Y = 0.4290*X + 8.698	0.3570	0.0054
	Y RS–SSNi vs. height	Y = 0.3089*X - 23.65	0.2080	0.0433
B	X LA–SSNi vs. spine length	Y = 0.3666*X + 29.39	0.1968	0.0500
	Y LA–SSNi vs. spine length	Y = 0.5230*X - 7.837	0.3324	0.0078
C	X LA–SSNi vs. width	Y = 0.4223*X + 6.077	0.3345	0.0076
	Y LA–SSNi vs. width	Y = 0.3555*X - 30.75	0.2450	0.0265

X RS–SSNi: Lateral distance from root of scapular spine to average infraspinatus motor point

Y RS–SSNi: Inferior distance from root of scapular spine to average infraspinatus motor point

X LA–SSNi: Medial distance from lateral acromion to average infraspinatus motor point

Y LA–SSNi: Inferior distance from lateral acromion to average infraspinatus motor point

Summary statistics of simple linear regression analysing the relationship between the average motor nerve entry into infraspinatus (SSNi) and scapular dimensions.

This suggests that for certain landmarks, patient-specific scapular dimensions can be used to inform injection approaches to target supraspinatus and infraspinatus motor points. This notion was anatomically validated via blind methylene blue dye injections into four additional shoulder specimens, distinct from the original sample.

Development and Preclinical Validation of a Landmark-Guided Injection Protocol

To simulate clinically translatable, landmark-guided injections, the following procedural steps were undertaken to validate the accuracy of targeting supraspinatus and infraspinatus motor points:

1. Measurement of Scapular Dimensions
Each shoulder specimen with intact skin overlying the supraspinatus and infraspinatus was measured for scapular height, spine length, and width. These measures were used to personalise the injection approaches. All three scapular dimensions yielded near identical predicted distances for injection targeting. Scapular spine length was selected for presentation due to its simplicity and ease of measurement.

2. Application of Patient-Specific Predictive Models
The recorded scapular spine lengths were inputted into linear regression equations derived from dissected specimens (see *Results*, Tables 4 and 5) to generate predicted coordinates for the average site of supraspinatus motor points.

- For supraspinatus injection, two distances were calculated:
    - X-distance from the root of the scapular spine (medial–lateral)
        - *[equation: X-distance = 0.3595*(spine length) - 29.76]*
    - Y-distance from the deltoid tubercle (anterior–posterior)
        - *[equation: Z-distance = 0.6444*(spine length) - 23.85]*

These values defined the relative projected coordinate of the average supraspinatus motor point (injection target) deep to the skin surface and trapezius (Figure 9A).

- For infraspinatus, lateral acromion was used as a single reference point. The root of the scapular spine could also have been used, but the authors found that lateral acromion was more easily palpable in specimens of variable adiposity or muscularity. The corresponding X (medial-lateral) and Y (superior-inferior) distances were calculated based on scapular spine length to localise the predicted average motor point for injection:

- X (medial-lateral) and Y (superior-inferior) distances from the lateral acromion
  - *[equations: X-distance = 0.3666*(spine length) + 29.39*
    Y-distance = 0.5230(spine length) - 7.837]*

These values defined the relative projected coordinate of the average infraspinatus motor point (injection target) deep to the skin surface and deltoid (Figure 8B).

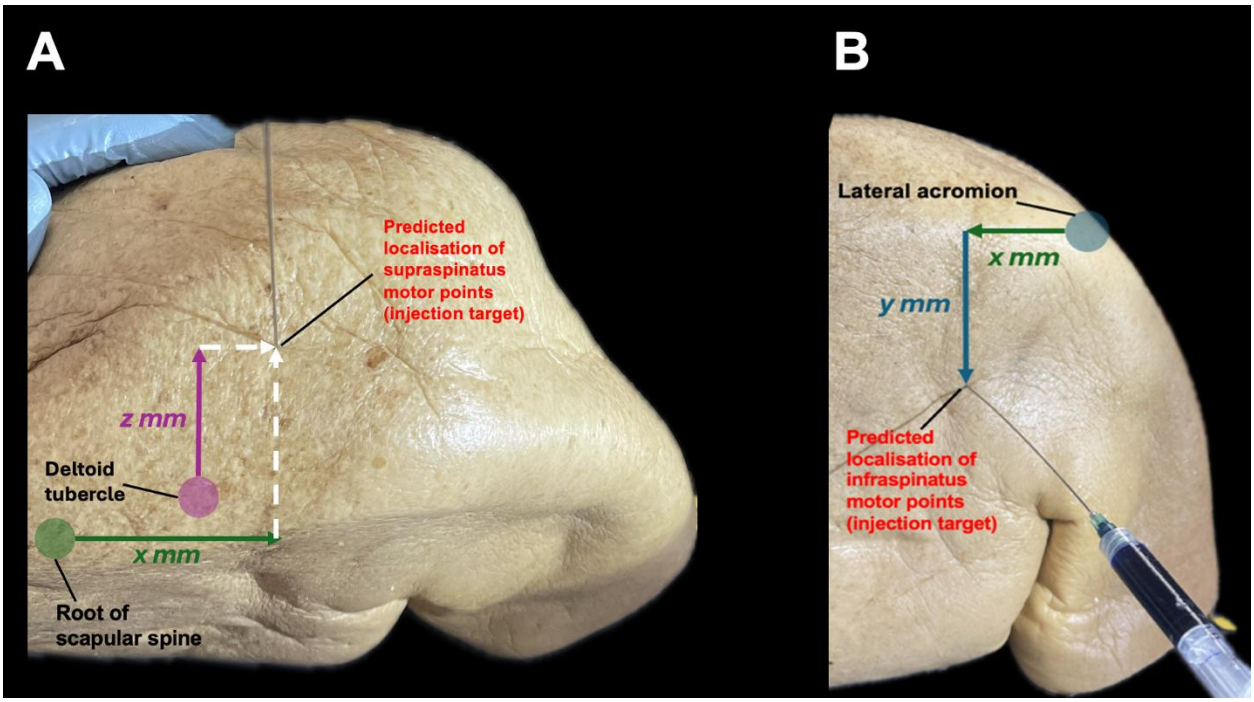

Figure 8. Landmark-guided approaches for injecting supraspinatus and infraspinatus

A) superior view of right shoulder demonstrating the injection approach for supraspinatus. B) posterior view of right shoulder demonstrating injection approach for infraspinatus.

3. Landmark-Guided Injection Technique

The defined injection sites were marked on the skin surface using the calculated distances from the relevant palpated bony landmarks. A 25-gauge needle was inserted perpendicular to the skin at the predicted coordinate and advanced until resistance indicated contact with the underlying bony floor of the supraspinous or infraspinous

fossa, simulating clinical depth. A volume of 2.5 mL of 0.25% methylene blue dye was injected to simulate BoNT delivery.

This image-free, patient-specific protocol enabled consistent and anatomically accurate targeting of supraspinatus and infraspinatus motor points, as validated through post-injection dissection. All four specimens demonstrated complete coverage of both supraspinatus and infraspinatus motor points (Figure 9).

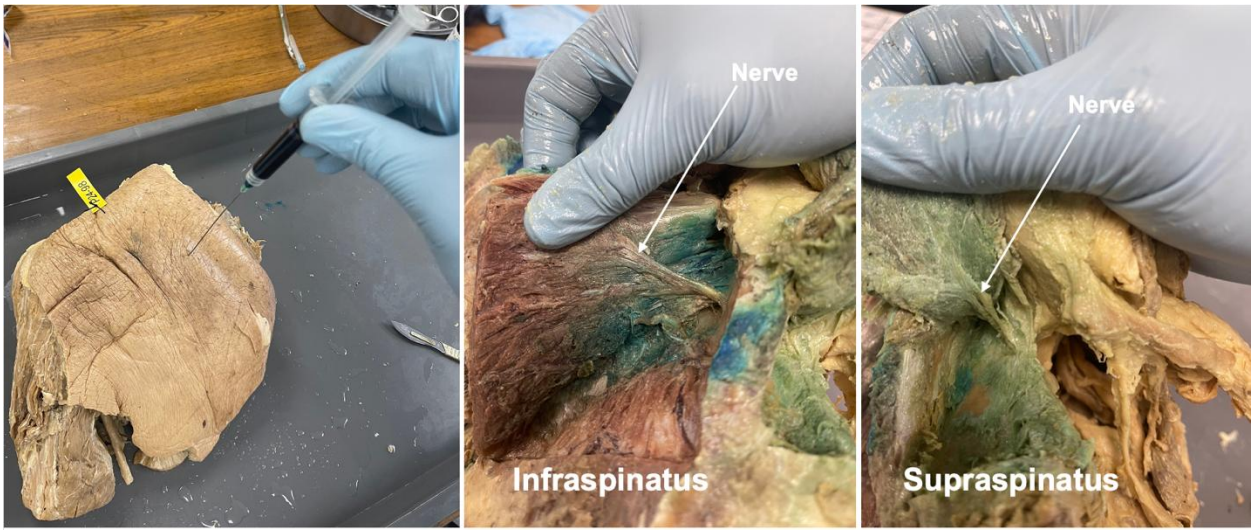

Figure 9. Dye injection validation on a left shoulder specimen showing coverage of both infraspinatus and supraspinatus motor points

Example of a left shoulder specimen injected by methylene blue dye to target supraspinatus and infraspinatus motor points. Figure shows injection of infraspinatus, sufficient dye coverage of motor points of both infraspinatus and supraspinatus based on patient-specific, landmark-guided injection.

Discussion

This cadaveric study demonstrates that patient-specific scapular dimensions can predict the topographical location of supraspinatus and infraspinatus motor points. Harnessing this finding, we propose a novel landmark-guided approach for botulinum neurotoxin (BoNT) injection into these muscles. In this approach, the needle is injected a defined distance from palpable scapular landmarks to reach the predicted motor points. These distances are patient-specific, informed by scapular size, easily measurable in clinic. This approach enables image-free targeting of motor points and was validated via successful dye injection in all specimens tested.

Anatomical studies have suggested variability in the topography of supraspinatus and infraspinatus motor points (Lee et al., 2022, 2023). Through mapping these motor points, these studies developed ultrasound-guided injection techniques for BoNT delivery. Alongside electromyographic guidance, ultrasound-guided BoNT injections are imperative in treating myofascial pain (Evans and Porter, 2015; Tan and Jia, 2021). However, such modalities are not universally available, particularly in low-resource settings (Becker et al., 2016). Another approach to BoNT delivery for myofascial pain involves tender point palpation and blind injection where the skeletal muscle band is most tender and taut (Climent et al., 2013). However, this technique has shown limited long-term success in treating pain (Hollingworth et al., 1983; Rubin et al., 2009).

Our study establishes reproducible, landmark-guided approaches that do not require specialist equipment, are anatomically validated, and are patient-specific. The technique relies on measurements in two anatomical axes relative to palpable landmarks. This confers directional specificity that enables clinicians to determine where to inject in relation to scapular landmarks.

These findings have important implications for improving the precision of BoNT injections. The therapeutic effect of BoNT is dependent on its proximity to motor endplates, approximately where motor nerves enter muscle (Harrison et al., 2007) (Miguel and Cirera, 2021). By localising these motor points via palpable scapular

landmarks, our method may allow more accessible and standardised delivery of BoNT injections.

Numerous scapular landmarks showed utility in guiding intramuscular BoNT injections into the rotator cuff, such as the root of the scapular spine, deltoid tubercle, and lateral acromion. In particular, the deltoid tubercle represents a landmark not previously exploited or appreciated in injection planning.

Validation using 2.5 mL methylene blue injections confirmed the accuracy of our proposed landmark-guided injections. This injectate volume is comparable to clinical volumes, suggesting high translational potential. Further enhanced motor point targeting could reduce required dosages, lower costs and minimise off-target effects such as unwanted paralysis (Carré et al., 2024). The landmark-guided approaches may also be relevant for intramuscular lidocaine or corticosteroid injections in managing rotor cuff pain of myofascial or neurogenic (e.g. hemiplegic shoulder) origin (Anwar et al., 2024).

Via the findings from this study, we proposed a protocol for performing BoNT injections, guided by patient-specific anatomy and scapular landmarks. Scapular spine length provides a practical reference for personalising injections, though height and width offer comparable utility. All are readily measurable via surface palpation.

Nevertheless, the findings yield important clinical considerations:

- Scapular dimensions allow for patient-specific adjustments, supporting personalised medicine.
- This technique may be especially useful in settings lacking ultrasound, or electromyography.
- Injection depth (not informed by the present study) should be adjusted based on individual patient anatomy, accounting for variation in subcutaneous fat, muscle bulk, and scapular contour.
    - In patients with greater muscle bulk, a deeper insertion may be required.
    - In frail or elderly patients, inject more superficially.

- With the growing adoption of automation in medicine, the study's linear equations could support future development of algorithmic injection guides or point-of-care tools.

Limitations and Future Directions

Despite the strengths of this study, several limitations should be acknowledged. The use of elderly, formalin fixed cadaveric specimens may not reflect the tissue characteristics of younger patients *in vivo;* fresh frozen specimens are thought to better resemble the living state and may have offered greater utility (Jansen et al., 2020). However, muscle atrophy and post-fixation shrinkage, coupled with the lack of blood flow, may still have altered the spread of injectate compared to the *in vivo* state (Tran et al., 2015). Furthermore, just 10 unique individuals (20 shoulders) were included to generate the injection approaches, indicative of a small sample size. Similarly, the restricted dye validation sample (n=4) is a limitation, even though all demonstrated accurate coverage. In addition, we did not include a dry bone validation cohort. Such an approach–or comparable radiological validation using CT or MRI–could strengthen reproducibility testing by confirming the reliability of scapular landmarks across larger and more diverse populations. This is an avenue for future investigation. Moreover, while we correlated sites of anatomical motor points with scapular dimensions, we could not confirm functional motor endplate activity with electromyography. In the future, this scapular dimension-informed, landmark-guided localisation of suprascapular nerve motor endplates could be confirmed in living patients via both electromyography and ultrasound.

This anatomical framework for patient-specific injections could be extended beyond the rotator cuff to other muscles with defined motor points. Moreover, some studies suggest multiple injections, rather than a single injection, into infraspinatus may improve outcomes (Lim et al., 2008); therefore, a dual-point injection strategy, informed by landmarks, could be explored.

Conclusion

This study presents the first pre-clinically validated, patient-specific, landmark-guided approach for intramuscular BoNT injection into the rotator cuff. By leveraging predictable correlations between scapular dimensions and the topography of supraspinatus and infraspinatus motor points, our approach enables accurate, image-free injection targeting with broad clinical utility. These findings represent a translational step towards more accessible and precise treatment of shoulder pain.

References

Anwar N, Wei X, Jie Y, Hongbo Z, Jin H, Zhu Z. 2024. Current advances in the treatment of myofascial pain syndrome with trigger point injections: A review. Medicine (Baltimore) 103:e39885.

Becker DM, Tafoya CA, Becker SL, Kruger GH, Tafoya MJ, Becker TK. 2016. The use of portable ultrasound devices in low- and middle-income countries: a systematic review of the literature. Trop Med Int Health 21:294–311.

Bron C, Gast A de, Dommerholt J, Stegenga B, Wensing M, Oostendorp RA. 2011. Treatment of myofascial trigger points in patients with chronic shoulder pain: a randomized, controlled trial. BMC Medicine 9:8.

Brox JI. 2003. Shoulder pain. Best Practice & Research Clinical Rheumatology 17:33–56.

Carré F, Amar J, Tankéré F, Foirest C. 2024. Botulinum Toxin Injections to Manage Sequelae of Peripheral Facial Palsy. Toxins (Basel) 16.

Cheshire WP, Abashian SW, Mann DJ. 1994. Botulinum toxin in the treatment of myofascial pain syndrome. PAIN 59.

Chu J. 1995. Dry needling (intramuscular stimulation) in myofascial pain related to lumbosacral radiculopathy. European journal of physical medicine & rehabilitation 5:106–121.

Climent JM, Kuan T-S, Fenollosa P, Martin-Del-Rosario F. 2013. Botulinum toxin for the treatment of myofascial pain syndromes involving the neck and back: a review from a clinical perspective. Evid Based Complement Alternat Med 2013:381459.

De Andrés J, Cerda-Olmedo G, Valía JC, Monsalve V, Lopez-Alarcón, Minguez A. 2003. Use of Botulinum Toxin in the Treatment of Chronic Myofascial Pain. The Clinical Journal of Pain 19.

Epstein S, Sparer EH, Tran BN, Ruan QZ, Dennerlein JT, Singhal D, Lee BT. 2018. Prevalence of Work-Related Musculoskeletal Disorders Among Surgeons and Interventionalists: A Systematic Review and Meta-analysis. JAMA Surgery 153:e174947–e174947.

Evans SF, Porter JM. 2015. Simplified technique for injection of Botulinum Toxin to Obturator Internus muscle using ultrasound-guided nerve stimulation for persistent pelvic pain. Aust NZ J Obst Gynaeco 55:612–614.

Gilchrist A, Pokorná A. 2021. Prevalence of musculoskeletal low back pain among registered nurses: Results of an online survey. Journal of Clinical Nursing 30:1675–1683.

Hains G, Descarreaux M, Hains F. 2010. Chronic Shoulder Pain of Myofascial Origin: A Randomized Clinical Trial Using Ischemic Compression Therapy. Journal of Manipulative and Physiological Therapeutics 33:362–369.

Harrison TP, Sadnicka A, Eastwood DM. 2007. Motor Points for the Neuromuscular Blockade of the Subscapularis Muscle. Archives of Physical Medicine and Rehabilitation 88:295–297.

Hollingworth GR, Ellis RM, Hattersley TS. 1983. Comparison of injection techniques for shoulder pain: results of a double blind, randomised study. Br Med J (Clin Res Ed) 287:1339–1341.

Jansen MM, Hazenberg CEVB, Ruiter QMB de, Hamersvelt RW van, Bleys RLAW, Herwaarden JA van. 2020. Feasibility of fresh frozen human cadavers as a research and training model for endovascular image guided interventions. PLoS ONE 15.

Kang J, Kim J, Park S, Paek S, Kim T, Kim D. 2019. Feasibility of Ultrasound-Guided Trigger Point Injection in Patients with Myofascial Pain Syndrome. Healthcare 7:118.

Kyu-Ho Yi, Ji-Hyun Lee, Hyun-Jun Park, Hyungkyu Bae, Kangwoo Lee, Hee-Jin Kim. 2023. Novel anatomical guidelines for botulinum neurotoxin injection in the mentalis muscle: a review. Anat Cell Biol 56:293–298.

Lee H-J, Lee J-H, Yi K-H, Kim H-J. 2022. Intramuscular Innervation of the Supraspinatus Muscle Assessed Using Sihler's Staining: Potential Application in Myofascial Pain Syndrome. Toxins 14:310.

Lee HJ, Lee JH, Yi KH, Kim HJ. 2023. Anatomical analysis of the motor endplate zones of the suprascapular nerve to the infraspinatus muscle and its clinical significance in managing pain disorder. Journal of Anatomy 243:467–474.

Lim JY, Koh JH, Paik NJ. 2008. Intramuscular botulinum toxin-A reduces hemiplegic shoulder pain: A randomized, double-blind, comparative study versus intraarticular triamcinolone acetonide. Stroke 39:126–131.

Miguel C, Cirera A. 2021. Retrospective study of the clinical effect of incobotulinumtoxinA for the management of myofascial pain syndrome in refractory patients. Toxicon 203:117–120.

Perez-Palomares S, Oliván-Blázquez B, Arnal-Burró AM, Mayoral-Del Moral O, Gaspar-Calvo E, Beldarraín ML de-la-Torre-, López-Lapeña E, Pérez-Benito M, Ara-Loriente V, Romo-Calvo L. 2009. Contributions of myofascial pain in diagnosis and treatment of shoulder pain. A randomized control trial. BMC Musculoskeletal Disorders 10:92.

Rubin TK, Gandevia SC, Henderson LA, Macefield VG. 2009. Effects of Intramuscular Anesthesia on the Expression of Primary and Referred Pain Induced by Intramuscular Injection of Hypertonic Saline. The Journal of Pain 10:829–835.

Shapiro SS, Wilk MB. 1965. An Analysis of Variance Test for Normality (Complete Samples). Biometrika 52:591–611.

Shin HJ, Shin JC, Kim WS, Chang WH, Lee SC. 2014. Application of Ultrasound-Guided Trigger Point Injection for Myofascial Trigger Points in the Subscapularis and Pectoralis Muscles to Post-Mastectomy Patients: A Pilot Study. Yonsei Med J 55:792.

Simons DG, Hong C-Z, Simons LS. 2002. Endplate Potentials Are Common to Midfiber Myofacial Trigger Points. American Journal of Physical Medicine & Rehabilitation 81:212–222.

Tan B, Jia L. 2021. Ultrasound-Guided BoNT-A (Botulinum Toxin A) Injection Into the Subscapularis for Hemiplegic Shoulder Pain: A Randomized, Double-Blind, Placebo-Controlled Trial. Stroke 52:3759–3767.

Tran T, Sundaram CP, Bahler CD, Eble JN, Grignon DJ, Monn MF, Simper NB, Cheng L. 2015. Correcting the Shrinkage Effects of Formalin Fixation and Tissue Processing for Renal Tumors: toward Standardization of Pathological Reporting of Tumor Size. Journal of Cancer 6:759–66.

Villafañe JH, Lopez-Royo MP, Herrero P, Valdes K, Cantero-Téllez R, Pedersini P, Negrini S. 2019. Prevalence of Myofascial Trigger Points in Poststroke Patients With Painful Shoulders: A Cross-Sectional Study. PM & R : the journal of injury, function, and rehabilitation 11:1077–1082.

Xie P, Qin B, Yang F, Yu T, Yu J, Wang J, Zheng H. 2015. Lidocaine Injection in the IntramuscularInnervation Zone Can Effectively Treat ChronicNeck Pain Caused by MTrPs in the TrapeziusMuscle. Pain Phys 5;18:E815–E826.